Ionic liquid mediated urea pyrolysis to cyanuric acid: Experimental protocol and mechanistic insights

Yusif Abdullayev*[a, b], Valentina Javadova^{[a], †}, Isa Valiyev^{[c], †}, Avtandil Talybov^[b], Cavanshir Salmanov^[a], and Jochen Autschbach^[d]

- [a] Department of Chemical Engineering, Baku Engineering University, Hasan Aliyev str. 120, Baku, Absheron, AZ0101, Azerbaijan
- [b] Institute of Petrochemical Processes, Azerbaijan National Academy of Sciences, Hojaly ave. 30, AZ1025, Baku, Azerbaijan
- [c] Department of Chemistry and Biology, University of Siegen, Adolf-Reichwein str. 2, D-57068, Siegen, Germany
- [d] Department of Chemistry, University at Buffalo, State University of New York, Buffalo, New York 14260-3000, United States

E-mail: <u>yabdullayev@beu.edu.az</u> Supporting Information Placeholder

ABSTRACT: Cyanuric acid **(CA)** is a critical precursor preventing the photodegradation of chlorine in water. So mainly, **CA** is utilized in the industry as a chlorine stabilizer. Compared to urea, the higher cost of **CA** necessitates an economic protocol to produce. As an alternative to current methods, we proposed dimethyl ammonium hydrosulfate [dmaH][HSO₄] ionic liquid (IL) mediated urea pyrolysis to **CA** for the first time. The reaction was optimized based on changing parameters: time, catalyst loading, solvent, and temperature. The optimized method does not require solvent utilization; IL acts as a solvent/catalyst system to produce **CA** in a \sim 70% yield at 220 °C in 30 min. The recycle test of IL catalyst shows that it can be reused four times without the loss of catalytic activity.

The IL catalytic activities on the urea pyrolysis reaction are studied using Density Functional Theory (DFT). The reaction profile of urea conversion to **CA** is calculated to follow biuret, triuret, and triuret cyclization steps, with extrusion of ammonia in each step. The IL-free reaction profile (Figure 6, green route) is also included to observe the IL role in the reaction. Considering experimental observation of isocyanic acid (**ICA**) as one of the urea pyrolysis products, we also tested **CA** formation possibilities via **ICA** trimerization. The calculations show that **ICA** formation (**TS-ICA**, ΔG^{\ddagger} =27.1 kcal/mol) is 14.1 kcal lower than biuret formation (**TS-I-IL**, ΔG^{\ddagger} =41.2 kcal/mol). Further mechanistic studies imply urea pyrolysis to **CA** follows a straightforward **ICA** trimerization route (Figure 8 and Scheme 4).

1. Introduction

The cyanuric acid (CA) market was valued at USD 367.9 million in 2020 and is expected to grow and reach USD 439.6 million by 2027, according to a report (Global cyanuric acid market outlook 2022). Because of the huge industrial utilization of CA to produce trichloroisocyanuric acid (TCCA), sodium dichloroisocyanurate (SDIC), and fire-retardant material (Figure 1), CA has reached such an enormous market value.

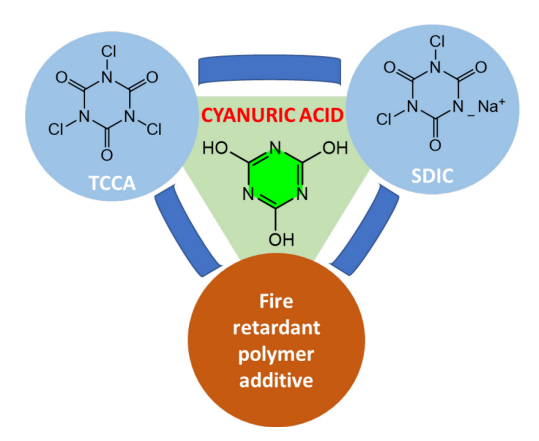


Figure 1. Product distribution from the industrial level CA conversion.

TCCA and SDIC are highly effective disinfectants against almost all types of bacteria, and viruses, including HIV, so the

compounds are gradually replacing traditional bleaches like liquid chlorine, sodium hypochlorite, and calcium hypochlorite. TCCA was used as a reagent for the efficient halogenation of aromatic and carbonyl compounds and as a catalyst to obtain amides from amines and aldehydes at room temperature.

Melamine-cyanuric acid complex (MCA) was utilized as a "greener" additive to obtain the halogen-free flame retardant MCA/Nylon 66 composites by melt blending technique.6 Thermal polycondensation of the MCA under nitrogen at 550 °C resulted in the formation of graphitic carbon nitride mesoporous hollow spheres, which are excellent nonmetallic catalysis for organic photosynthesis, solar energy conversion, and photodegradation of waste materials.^{7, 8} CA as an organocatalyst was applied to convert carbon dioxide into oxazolidinones and quinazolines at room temperature and atmospheric pressure.⁹ MCA complex was exploited for facile palladium recovery from an aqueous solution. Then Pd was separated quantitatively from the formed Pd-MCA complex.¹⁰

The **CA** large-scale utilization necessitates facile synthetic protocol, which has been a focus of scientists for the last four decades: Wang and co-workers proposed catalytic pyrolysis of urea on the surface of V-Ti catalyst to biuret, melamine, and **CA**.¹¹ The thermal decomposition of urea was studied in an open vessel, and it was identified that the **CA** yield reaches a maximum at 250 °C.¹² A systematic study was conducted on the urea pyrolysis under nitrogen to **CA** and the carbon nitride-based semiconductive material.¹³ Jeilani *et al.* studied

prebiotic-assisted synthesis of melamine, ammeline, ammelide, and **CA** from urea, and they predicted the reaction mechanism with density functional theory (DFT).¹⁴ In the absence of water and organic solvents, urea was converted to **CA** using microwave-assisted heating.¹⁵ Tischer *et al.* conducted thermodynamic and numeric studies on the urea decomposition kinetics to biuret, triuret, and **CA**.¹⁶ **CA** synthesis from urea was tested in various solvents and the presence of Lewis acidic catalysts. It was found that kerosene and diesel are reasonable solvents to proceed the reaction in relatively mild conditions (180 °C) to obtain **CA** in a high yield (88%), and using Lewis acidic catalysts did not contribute to increase the yield.¹⁷ The industrial production of **CA** generally relies on sulfuric acid catalyzed urea pyrolysis process.^{18, 19}

Extensive **CA** utilization in the industry necessitates developing facile and environmentally benign synthetic procedures. Most previous studies show that using toxic and expensive solvents and catalysts makes urea pyrolysis challenging for industrial applications. The utilization of sulfuric acid for industrial **CA** production required building another unit to neutralize excess ammonia, which resulted in a significant increase in production cost.²⁰ Therefore, replacing highly corrosive sulfuric acid with mild and "greener" alternatives, such as low-cost ionic liquid (IL) can be a preferred option for urea pyrolysis.

Theoretical studies were applied to understand reaction mechanisms and direct experimentalists to design an efficient catalyst, eventually developing a cost-effective procedure. ^{21, 22} Despite the industrial importance of the reaction (Scheme 1), only a few computational studies were performed on the catalyst-free urea pyrolysis. ¹⁴ Parallel to experimental optimizations, we theoretically studied the urea pyrolysis mechanism. Direct urea trimerization to **CA** in the presence of IL catalyst and catalyst-free conditions (Figure 6) were investigated. Considering urea decomposition to **ICA**, its trimerization to **CA** was tested twice in catalyst-free and catalytic conditions.

To the best of our knowledge, for the first time, we propose to utilize IL as a solvent/catalyst system to convert urea into **CA** according to the following scheme (Scheme 1).

Scheme 1. IL mediated urea pyrolysis reaction.

2. Experimental

2.1 Synthesis and characterization of ILs. Urea was purchased from Thermo Fisher Scientific in 98% purity for the synthesis. [maH][HSO₄] was purchased from abcr GmbH in 97% purity; [bmim][BF₄] and [bmim][PF₆] were purchased from Iolitec Ionic Liquids Technologies in 99% purity. The other ILs described in Table 2 were synthesized according to known procedures.²³ The spectral data of these compounds are in good agreement with those in the literature reports.

2.2 Synthesis and characterization of products. Synthesis of **CA** was carried out in one necked round bottom flask (25 ml); IL and urea 5:1, (w:w) respectively were added to the flask with a magnetic stirring bar. The reaction was conducted at 220 °C for 30 min, then ice-cooled for 10 min, transferred to the deionized icy water (100 ml) beaker, and stirred for 3 min to remove the catalyst residue. The organic precipitation was collected via filtration and washed with deionized icy water

(100 ml). After filtration, the precipitate dried at 45 °C in a vacuum oven overnight. Without further purification, the product was subjected to NMR, elemental analysis, ESI-MS, FT-IR, and melting point (ESI, Page S05). The reaction condition for the recycle test is the same as the above-mentioned procedure. The catalyst recovery was conducted as follows: After separation of the precipitate, the aqueous layer was washed with diethyl ether (5x100 ml) and evaporated, and the obtained catalyst residue in water was dried under low pressure at 50 °C for the next use.

3. Computational Details

The Gaussian 16 package was used in all calculations.²⁴ Molecular geometries of all species were optimized via exploiting DFT/B3LYP functional^{25, 26} with Grimme's empirical dispersion correction (D3).27 6-31G* basis sets were used for H, C, N, and O atoms. For S and K atoms, the 6-31++G(d,p) basis was exploited according to recent recommendations.28 The reaction was calculated based on the experimental reaction conditions (1 atm, 493.15 K) in the gas phase. Self-consistent reaction field (SCRF) with dielectric constants for DMSO (ϵ = 46.7) and DMF (ε = 37.2) were exploited to recalculate (1 atm, 393.15 K) green route of Figure 8. It was found that applying a solvation model does not significantly change the energy barriers of the IL-mediated ICA trimerization cycle (ESI, Table S6 and S7). An intrinsic reaction coordinate (IRC) search was executed to confirm the obtained transition states (one imaginary frequency) connected to intermediates (zero imaginary frequency) structures. All the intermediate and transition state structures were calculated without geometry constraints. Optimized Cartesian coordinates, total energies, Gibbs energies, and enthalpies of all structures are provided in supporting information (ESI).

4. Results and discussion

4.1 Variation of the solvent. The yield investigation of the urea pyrolysis to CA was performed based on five variables: type of ILs, catalyst (IL) loading, reaction temperature, reaction time, and solvents. The highest yield (68 ± 2%) of CA was observed in the neat conditions in the presence of [dmaH][HSO₄], (IL: Urea; 5:1, w:w) at 220 °C for 25-30 minutes. Solvents with high boiling points, i.e., naphthalene, nitrobenzene, ethylene glycol, and DMSO were tested on the reaction (Table 1) with constant solvent and IL ratio (1:1, w:w) to investigate the impact of solvent on the reaction yield. The solvent utilization does not contribute to the CA yield in all cases. All the tested solvents resulted in a similar moderate yield (60-68%) of CA except for DMSO: Only 35 (± 2)% of the product was isolated in the presence of DMSO. The excess solubility of the product may explain the sharp decline in the yield in DMSO compared to other solvents. Another reason for the product low yield may be scrutinized with the decomposition of DMSO at the applied high temperature (220 °C).29 Because of the good solubility of **CA** in the DMSO + IL mixture, further purification of the product becomes challenging. The reaction mixture was kept (in the case of DMSO) at -5 °C for 8 h to precipitate CA quantitatively, which is simultaneously happening when we cool the reaction mixture in the case of other utilized solvents. As seen in Table 1, exploiting nitrobenzene and ethylene glycol resulted in a very close isolated yield of 60 (±2) %. The observation shows that IL as a solvent is a good option for the urea pyrolysis to CA. Accordingly, further studies have been carried out with the presence of only IL as a solvent/catalyst to promote the reaction.

Entry	Solvent : IL (1 : 1, w : w)	Yield (%)
1	naphthalene : [dmaH][HSO ₄]	68
2	nitrobenzene : [dmaH][HSO ₄]	61
3	ethylene glycol : [dmaH][HSO ₄]	60
4	DMSO : [dmaH][HSO ₄]	35
5	: [dmaH][HSO ₄]	68

Table 1. The yields of **CA** versus various solvents in the presence of [dmaH][HSO₄] at 220 °C for 30 min (IL: Urea; 5:1, w:w).

4.2 Variation of the ionic liquid. The **CA** formation from urea is studied after 25 min at 220 °C in the presence of various (IL: Urea; 5:1, w:w) ILs (Table 2). Without an IL catalyst, a small urea conversion to **CA** was observed, 14 (± 2)%. The best results were achieved in the presence of [dmaH][HSO₄] and [deaH][HSO₄], 68 and 63 (± 2)%, respectively.

$\begin{array}{c} -N\overset{+}{\operatorname{NH}}_3\operatorname{HS}\bar{\operatorname{O}}_4\\ \\ \stackrel{+}{\operatorname{NH}}_2^{\prime}\operatorname{HS}\bar{\operatorname{O}}_4\\ \\ \stackrel{+}{\operatorname{NH}}_2^{\prime} \\ \end{array}$	Methylammonium hydrogen sulfate Dimethylammonium hydrogen sulfate	[maH][HSO ₄] [dmaH][HSO ₄]	68
^+^ -	Dimethylammonium	[dmaH][HSO ₄]	68
^+^ -	•	[dmaH][HSO ₄]	68
NH ₂ HSO ₄	hydrogen sulfate		
The HSO ₄			
	Diethylammonium	[deaH][HSO ₄]	63
	hydrogen sulfate		
HSC H ₂	Dibuthylammonium	[dbaH][HSO ₄]	50
	hydrogen sulfate		
N H ₂ HSO ₄	Diisobuthylammonium	[dibaH][HSO ₄]	45
	hydrogen sulfate		
HSO ₄	Diisopropylammonium hydrogen sulfate	[dipaH][HSO ₄]	50
N N $\bar{B}F_4$	1-butyl-3-methyl-	[bmim][BF ₄]	-
	imidazolium tetrafluoroborate		
N $\stackrel{+}{\sim}$ \overline{PF}_6	1-butyl-3-methyl-	[bmim][PF ₆]	-
	\vec{H}_2 \uparrow \uparrow \uparrow \downarrow \uparrow \downarrow \uparrow \downarrow \uparrow \downarrow \uparrow \downarrow \downarrow	Dibuthylammonium hydrogen sulfate H_2 HSO_4 Diisobuthylammonium hydrogen sulfate H_2 HSO_4 Diisobuthylammonium hydrogen sulfate H_2 Diisopropylammonium hydrogen sulfate H_2 H_3 H_4 Diisopropylammonium hydrogen sulfate 1-butyl-3-methyl-imidazolium tetrafluoroborate	$\begin{array}{cccccccccccccccccccccccccccccccccccc$

Table 2. Tested IL catalysts on urea pyrolysis reaction. The **CA** yield in the presence of various ILs at 220 °C for 30 min (IL: Urea; 5:1, w:w).

The CA yield declines when the number of carbon atoms at the amine part of IL increases. One possible reason for the change in the product yield is long-chain alkyl groups in the IL amine part, enhancing surfactant abilities (forming a foamlike mixture when the urea is added at high temperatures). The same case was not observed for IL [maH][HSO₄], [dmaH][HSO₄], and [deaH][HSO₄] with smaller alkyl chains. The long alkyl chain containing ILs, e.g., [dbaH][HSO₄] and [dibaH][HSO₄] form foam at the indicated temperature during the reaction period, which prevents effective mixing.30 The long-chain ILs steric effects may adversely impact catalytic activities. The IL [maH][HSO₄] with primary amine group shows less catalytic activity compared to the secondary amine group-containing IL [dmaH][HSO₄], which can be explained by the strong Lewis basicity of dimethylamine versus methylamine. In our previous experimental and computational works, we studied the secondary amine-containing [deaH][HSO₄] IL catalytic performance on a similar cyclocondensation reaction.31,32 It was found that both the basic and acidic parts of IL can act as a catalyst via proton exchange to promote cyclocondensation. The imidazolium salts are one of the most used ILs for their good catalytic activity,³³⁻³⁵ so we tested [bmim][BF4] and [bmim][PF6] ILs on the urea pyrolysis reaction, and unfortunately, no **CA** was isolated. Further optimizations were carried out in the presence of [dmaH][HSO4] as a catalyst because of the highest product yield.

4.3 Variation of the reaction time. The first set of reactions was performed at 220 °C with varying reaction times to obtain an indication of the reaction rate (Figure 2). According to Figure 2, the maximum CA yield (68 (± 2)%) is obtained at 25 and 30 min. After 25 min, the color of the reaction mixture was still white; however, at 30 min, turning the white color to pale yellow was observed. Running the reaction for the additional 15 minutes turned the color of the reaction mixture to brown, which turned to black when we kept the reaction running. The observations indicate the decomposition of the reaction components inside the reaction mixture. Because of the sharp decline of CA yield after 30 minutes, it can be proposed that CA is unstable and decomposes at the indicated temperature and time period. Analysis of the reaction mixture after running the reaction for 2 h shows no CA trace. This investigation shows that the yield is strongly time-dependent and can be tuned via time.

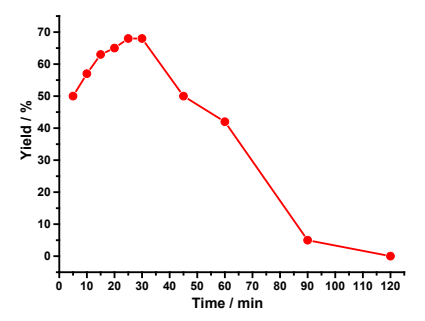


Figure 2. The **CA** yield versus time in the presence of [dmaH][HSO₄] at 220 °C (IL: Urea; 5:1, w:w).

4.4 Variation of the reaction temperature. The reaction is conducted at different temperatures in the presence of [dmaH][HSO₄] (IL: Urea; 5:1, w:w) in 30 min period (Figure 3). The **CA** yield increases with increasing temperature up to 220 °C, and beyond this point, CA formation declines significantly. CA formation is infinitesimal at temperatures lower than 170 °C and more than 270 °C. Previous studies are in good agreement with our experimental findings showing CA formation at the determined temperature range.15, 36 Such a high temperature (170 °C) requirement for selective urea pyrolysis to CA can be explained by the reaction high activation energy. It was scrutinized in the computational section (See Section 4.7). Beyond 220 °C, CA sublimation may be a primary reason for to decrease in the CA yield. Intensive sublimation of CA at a high temperature (>220 °C) was reported by Tischer et al.¹⁶

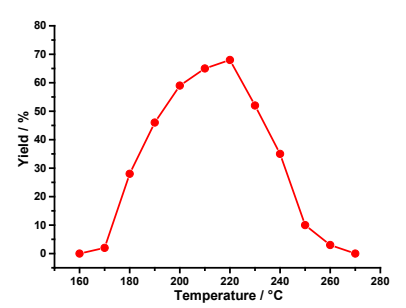


Figure 3. The **CA** yield versus temperature in the presence of [dmaH][HSO₄] for 30 min (IL: Urea; 5:1, w:w).

4.5 Variation of IL loading. The relation between different loadings of [dmaH][HSO₄] and product yields after 30 min of reaction time at 220 °C is given in Figure 4. As seen from the figure, conversion to the product increases from 1:1 to 5: 1 ratio loading. Between 5: 1 and 7: 1 ratios, the yield is the same and maximum (68 (± 2)%). With more than 7:1 ratio, the yield of the reaction starts to decline considerably. Above the 7:1 IL: urea ratio, IL starts to act as a solvent because of the noncovalent and electrostatic interactions between IL molecules. The presence of bulk IL decreases collision probability between IL and substrate molecules, resulting in a considerably low conversion of urea to CA. A detailed computational study was conducted in our previous work related to IL solvation versus catalysis that shed light on a similar case via comparing proton exchange and noncovalent interaction energy barriers on dehydration transition states.31

4.6 Recycle test. The IL [dmaH][HSO₄] recycle test over five cycles was performed for the urea pyrolysis reaction (IL : Urea; 5:1, w:w) at 220 °C for 30 min period. The catalyst preserves its effectiveness for four cycles, as seen in Figure 5. A slight decline in the **CA** yield (5%) was observed after the fifth run. The obtained recycle test results are satisfactory compared to the other homogeneous IL-promoted processes. 37,38

70-65-60-80-50-45-40-0 2 4 6 8 10 12 14 16 18 20 22 Ratio of IL : urea (N : 1)

Figure 4. The **CA** yield versus the amount of [dmaH][HSO₄] (**N**) at 220 $^{\circ}$ C for 30 min. The IL : urea ratio is based on w:w (IL : urea; N:1).

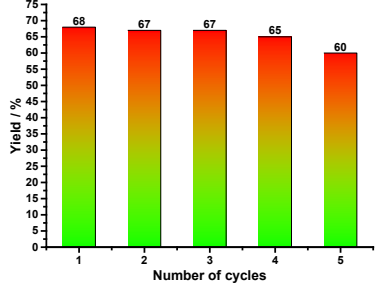


Figure 5. Recycle test of IL : [dmaH][HSO₄] (IL : Urea; 5:1, w:w); 220 °C; 30 min.

4.7 Mechanistic studies. We first calculated the IL-free route to see a clear picture of the IL role in the urea pyrolysis to **CA**. As seen in Figure 6 (green route), 61.9 kcal/mol energy is required to overcome the barrier (**TS1F**) for biuret (**I1F**) formation via ammonia extrusion. The addition of the next urea results in the formation of triuret (**I3F**), via a 59.2 kcal/mol (**TS2F**) energy barrier. Final cyclization of triuret (**TS3F**, $\Delta G^{\ddagger}=52.6$ kcal/mol) yields **CA**. The detailed mechanism for the IL-free route is shown in Scheme 2. The green route TSs were visualized and included in ESI (Figure S3).

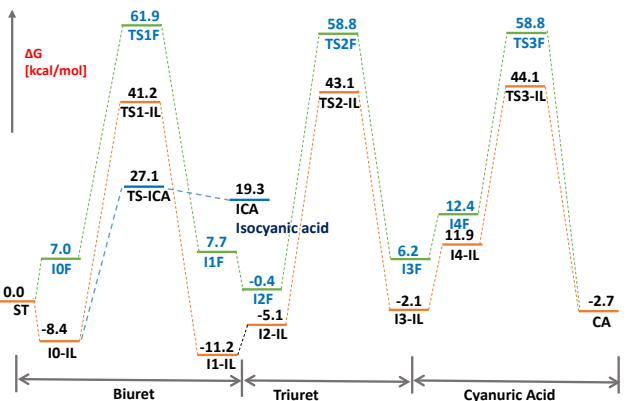
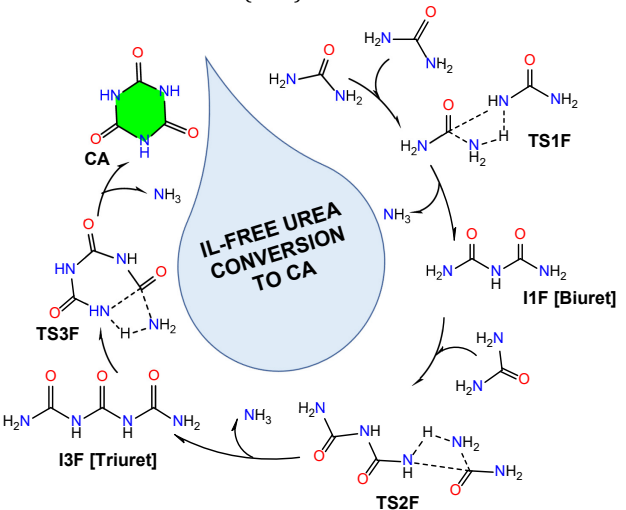


Figure 6. Energy profile for the urea pyrolysis to **CA**: IL-free route (green), IL-mediated urea conversion to **CA** (orange), IL-mediated **ICA** formation from urea (blue).



Scheme 2. Calculated mechanistic cycle of the urea pyrolysis to **CA** in the IL-free condition (Figure 6, green route).

The IL-free route with higher energy barriers shows that protonation, ammonia extrusion, and nucleophilic attack steps are challenging to proceed with, so we tested the same steps considering IL interactions with urea molecules.

IL catalysis route: As shown in Figure 6 (orange route) addition of a single IL molecule for proton exchange with substrate molecules results in significant decreases in energy barriers. Namely, the IL-mediated conversion of two urea molecules into biuret (I1-IL) is going through TS1-IL ($\Delta G^{\ddagger}=49.6 \text{ kcal/mol}$), which is 12.3 kcal/mol lower than the IL-free case. The triuret (I3-IL) formation path (TS2-IL) is also 4.9 kcal lower than the same path for the IL-free route.

The cyclization of **I3-IL** over ammonia extrusion is calculated to have a 46.3 kcal energy barrier that is 6.3 kcal lower than the IL-free path. The IL-mediated **CA** formation path TSs

are shown in Figure 7, with important bond parameters describing ammonia extrusion in each step.

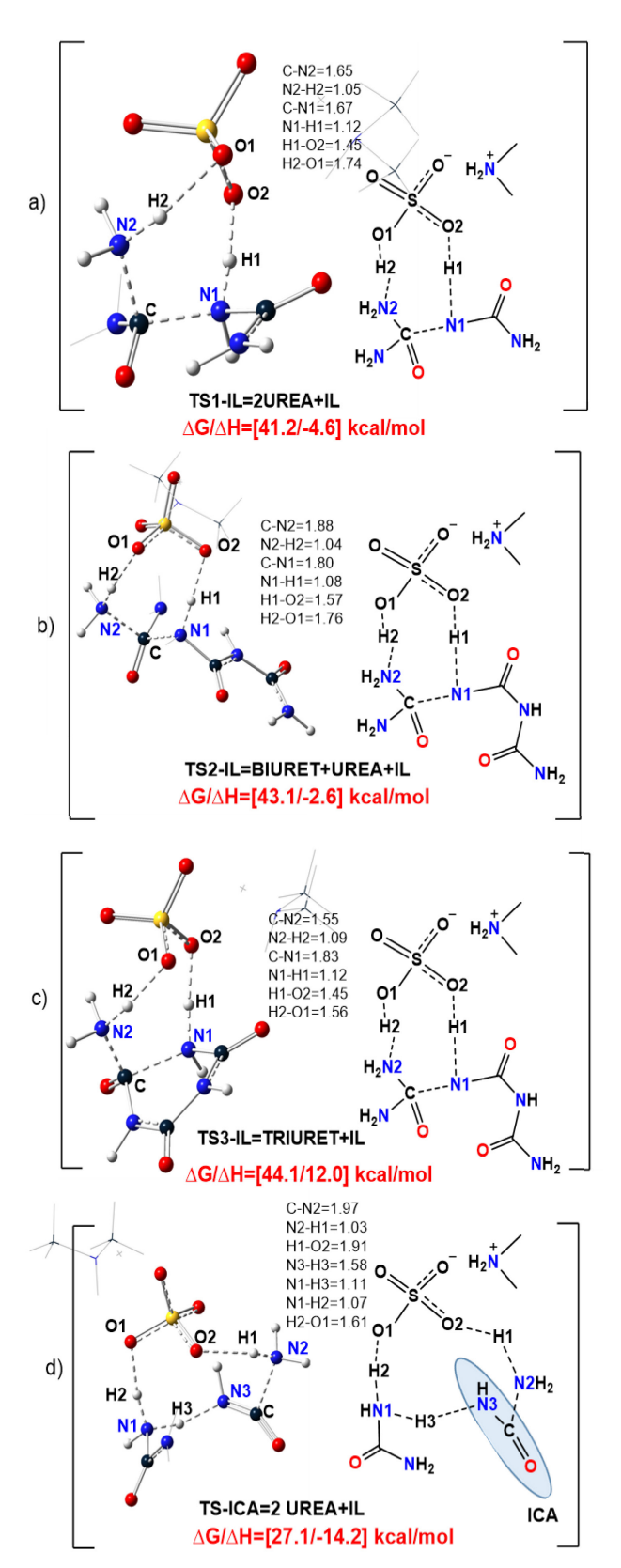
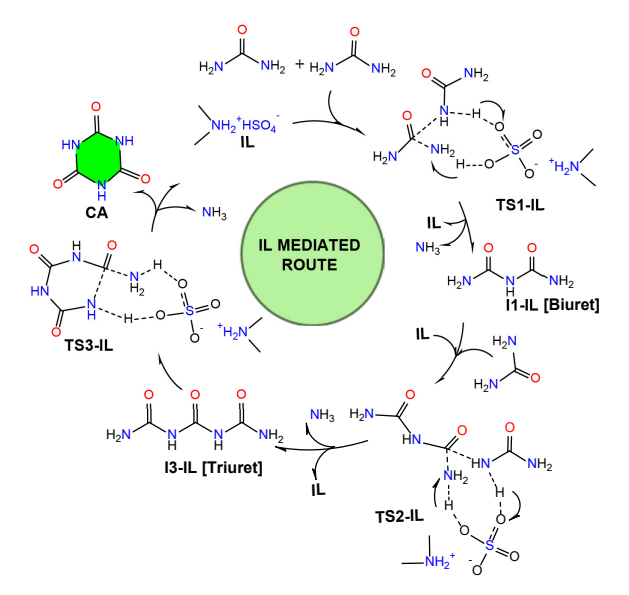


Figure 7. Optimized structures of TSs with important bond lengths (given in Å): a) **TS1-IL**, b) **TS2-IL**, c) **TS3-IL**, and d) **TS-ICA**. Some hydrogen atoms and the IL cation part are omitted to avoid clutter.

Ammonia extrusion is very critical in each step to maintain urea dimerization, trimerization, and eventually **CA** formation. As seen from the concerted **TS1-IL** structure (Figure 7), one of the urea -NH₂ (N2) groups accept a proton from IL (N2-H2: 1.05 Å), and the **C-N2** bond elongated up to 1.65 Å, which facilitates nucleophilic attack of the next urea (N1) to the electrophilic carbon (**C**) via 1.67 Å bond length. Eventually, simultaneous proton donation and acceptance from IL results in NH₃ extrusion; this scenario is replicated in the next two steps as **TS2-IL** and **TS3-IL**, yielding **CA**. The calculated mechanism of the IL-mediated urea pyrolysis is shown in Scheme 3 to understand better the IL role in the **CA** for-

Scheme 3, to understand better the IL role in the CA formation.

IL catalysis on ICA trimerization: It was experimentally evident that (with thermogravimetric and differential thermoanalysis) urea decomposition resulted in the formation of isocyanic acid (ICA) at 200 °C.11, 39, 40 Increased ICA concentration in the reaction mixture is supposed to be the main driving force to trigger **CA** formation via trimerization. So, it supports our experimental observations that why, above the 200 °C, the CA yield is maximum. Due to the fact we tried to calculate ICA trimerization to CA. First, IL-mediated ICA formation possibilities from urea were tested, and the related TS (Figure 7, TS-**ICA**) was successfully located. As seen from the TS structure, besides ammonia extrusion (C-N2, 1.97 Å), proton transfer (H3-N3, 1.58 Å) from the other urea NH₂- group is required to yield ICA structure. Unlike the urea coupling TSs (TS1-IL, TS2-IL, and TS3-IL), the urea NH₂- group is not acting like a nucleophile (N1); it acts as a base to abstract proton (H3) from the ICA adduct. The ICA formation energy barrier is significantly lower than (14.1 kcal) of the corresponding biuret (TS1-IL) energy barriers. Considering the solid fact, we decided the CA formation is possible via ICA trimerization.



Scheme 3. The calculated mechanistic cycle of the IL-mediated urea pyrolysis to **CA** (Figure 6, orange route).

As seen from the energy profile (Figure 8) that after the ICA formation (Figure 6, blue route), IL-mediated trimerization of ICA is straightforward with shallow energy barriers (green route). IL catalyst is more effective in the ICA case than the urea trimerization (Figure 8 green route vs. Figure 6 orange route). The IL catalyzed ICA dimerization step is calculated to be 23.6 kcal lower than the same route in the IL-free case (Figure 8, red route). The ICA trimerization (TS2-ICA-IL) is

calculated to have a 28.4 kcal/mol energy barrier, which is 29.6 kcal lower than the IL-free trimerization (TS2-ICA) barrier. The ICA trimer (I5-ICA-IL) is observed to yield CA without an energy barrier that requires 35.8 kcal/mol energy in the IL-free condition.

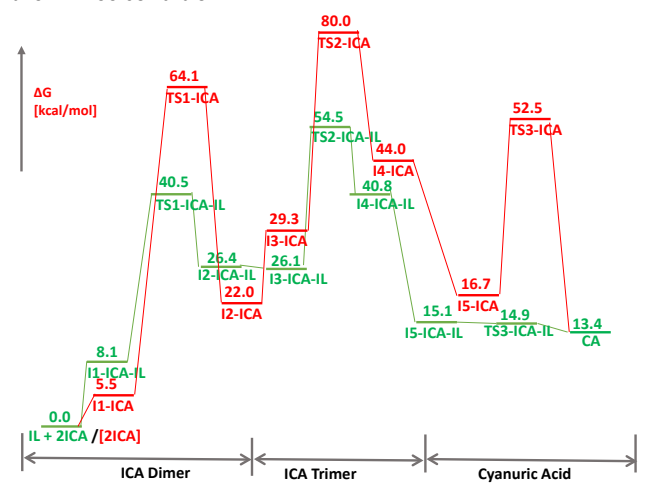
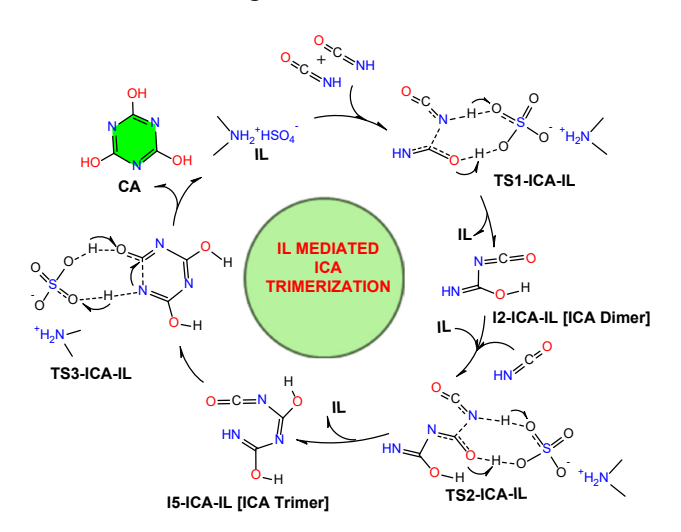


Figure 8. Energy profile for the **ICA** trimerization to **CA**: IL free route (red), IL mediated (green).

Based on our calculations and experimental evidence, it can be proposed that urea pyrolysis is likely to follow the **ICA** route to yield **CA**. The optimized structures of **ICA** dimerization, trimerization, and subsequent cyclization TSs were visualized and shown in Figure 9.



Scheme 4. The calculated mechanistic cycle of the IL-mediated **ICA** trimerization to **CA** (Figure 8, green route).

As seen from the **TS1-ICA-IL** structure, the nucleophilic attack of **ICA** nitrogen (N2) on electrophile (C1) via 1.81 Å is the main reason to yield **ICA** dimer. The attack is facilitated via protonation (H1-O3; 1.36 Å) of the carbonyl oxygen (O3). The deprotonated IL gains the **ICA** proton (H2) to retain its initial structure simultaneously (H2-O1; 1.10 Å). The same proton exchange and nucleophilic attack steps were replicated in **TS2-ICA-IL** and **TS3-ICA-IL** to form **CA** (Figure 9). The calculated mechanism for **ICA** trimerization and final cyclization steps is shown in Scheme 4.

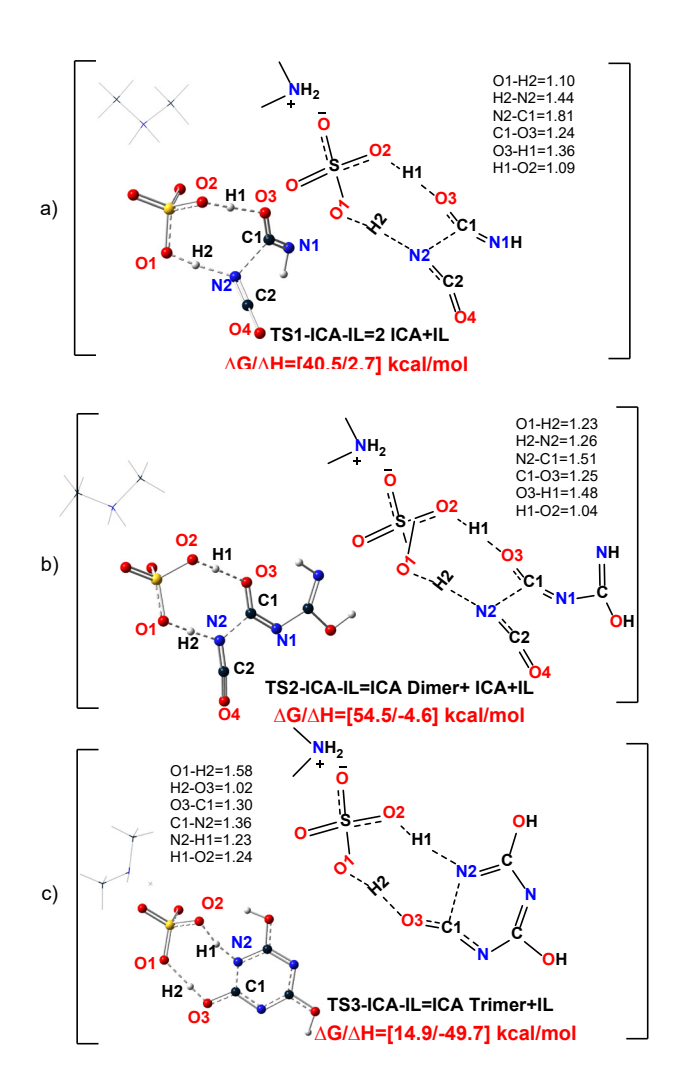


Figure 9. Optimized structures of TSs with important bond lengths (given in Å): a) **TS1-ICA-IL**, b) **TS3-ICA-IL**, and c) **TS2-ICA-IL**. Some hydrogen atoms and the IL cation part are omitted to avoid clutter.

The calculated IL-free ICA trimerization mechanism (Figure 8, red route) to CA is shown in ESI, (Scheme S1). Comparing the IL-free and IL-catalytic pathways of the reaction profile (Figure 8) of ICA trimerization to CA, the IL catalytic role is apparent. So, the urea pyrolysis reaction is more likely to follow IL catalyzed ICA trimerization mechanism (Scheme 4).

Conclusion

The low-cost IL-mediated urea pyrolysis to **CA** was studied experimentally and computationally. Experimental optimizations based on the time, temperature, solvent, and IL loading showed that ideal urea conversion to **CA** (~70% yield) was at 220 °C, in 30 min when IL: Urea ratio is 5:1 (w:w). The utilization of cheaper and 'greener' ionic liquid allowed to decrease the **CA** production cost because previously separate solvent and catalyst were used for the same reaction.¹⁷ The IL's low vapor pressure at 220 °C made it a superior solvent over traditional solvents and allowed it to conduct the reaction in an open flask. Additionally, the IL catalytic activities do not necessitate using a separate catalyst to boost conversion.

Detailed computational mechanistic studies were performed to scrutinize the IL catalysis of the reaction. The first

set of calculations followed urea conversion to biuret, triuret, and triuret cyclization to yield CA in IL-free and IL-catalysis conditions. As seen from Figure 6 and Scheme 2, the IL incorporation considerably declined energy barriers compared to IL-free (green path) route. Namely, biuret formation was 20.7 kcal lower in the case of IL-incorporated proton exchange compared to the IL-free case. The IL-incorporated triuret formation and cyclization steps were 15.7 kcal and 14.7 kcal lower relative to the IL-free condition. Our computation implied that the urea decomposition is more likely to go through ICA than biuret formation since the energy barrier of ICA formation is 14.1 kcal lower than the corresponding biuret formation TS (**TS1-IL**). Because of the shallow energy barriers compared to urea trimerization (Figure 6), the ICA trimerization was considered the best pathway to yield **CA**. The proposed IL-mediated urea pyrolysis to CA is not perfect, in particular, due to the moderate isolated CA yield (~70%), which can be enhanced via modifying the IL catalyst (using heterogeneous support for easier recovery and increasing turnover). The drawback was considered to be solved in our upcoming work. Compared to the previous studies, the work is bearing valuable contribution to the urea pyrolysis reaction, i.e., the solvent was eliminated, IL was applied, and the reaction mechanism was studied computationally in detail. The work promises an industrial perspective because of IL utilization as a 'greener' solvent/catalyst system for urea pyrolysis to CA.

ASSOCIATED CONTENT

Supporting Information

Full spectral characterization of cyanuric acid, and mechanistic studies data (PDF).

The Supporting Information is available free of charge on the ACS Publications website.

AUTHOR INFORMATION

Corresponding Author

*E-mail:yabdullayev@beu.edu.az

ORCID

Yusif Abdullayev: 0000-0003-0879-0062 Isa Valiyev: 0000-0001-6167-1594 Jochen Autschbach: 0000-0001-9392-877X Valentina Iavadova: 0000-0002-4651-538X

AUTHOR CONTRIBUTIONS

†Both authors contributed equally to the paper.

Notes

The authors declare no competing financial interest.

CONFLICTS OF INTEREST

There are no conflicts to declare

ACKNOWLEDGMENTS

Y.A. acknowledges the SOCAR Science Foundation, S/N 12LR-AMEA (05/01/2022). J.A. thanks The National Science Foundation, grant CHE 1855470, for support. All authors thank the Center for Computational Research (CCR) at the University at Buffalo for providing computational resources.

REFERENCES

- 1. Tilstam, U.; Weinmann, H., Trichloroisocyanuric Acid: A Safe and Efficient Oxidant. *Org. Process Res. Dev.* **2002**, *6* (4), 384-393.
- 2. Gaspa, S.; Carraro, M.; Pisano, L.; Porcheddu, A.; De Luca, L., Trichloroisocyanuric Acid: a Versatile and Efficient Chlorinating and Oxidizing Reagent. *Eur. J. Org. Chem.* **2019**, *2019* (22), 3544-3552.
- 3. Clasen, T.; Edmondson, P., Sodium dichloroisocyanurate (NaDCC) tablets as an alternative to sodium hypochlorite for the routine treatment of drinking water at the household level. *Int. J. Hyg. Environ. Health* **2006**, *209* (2), 173-181.
- 4. Mishra, A. K.; Nagarajaiah, H.; Moorthy, J. N., Trihaloisocyanuric Acids as Atom-Economic Reagents for Halogenation of Aromatics and Carbonyl Compounds in the Solid State by Ball Milling. *Eur. J. Org. Chem.* **2015**, *2015* (12), 2733-2738.
- 5. Yang, H.; Hu, W.; Deng, S.; Wu, T.; Cen, H.; Chen, Y.; Zhang, D.; Wang, B., Catalyst-free amidation of aldehyde with amine under mild conditions. *New J. Chem.* **2015**, *39* (8), 5912-5915.
- 6. Lu, X.; Qiao, X.; Yang, T.; Sun, K.; Chen, X., Preparation and properties of environmental friendly nonhalogen flame retardant melamine cyanurate/nylon 66 composites. *J. Appl. Polym. Sci.* **2011**, *122* (3), 1688-1697.
- 7. Jun, Y.-S.; Lee, E. Z.; Wang, X.; Hong, W. H.; Stucky, G. D.; Thomas, A., From Melamine-Cyanuric Acid Supramolecular Aggregates to Carbon Nitride Hollow Spheres. *Adv. Funct. Mater.* **2013**, *23* (29), 3661-3667.
- 8. Peng, G.; Xing, L.; Barrio, J.; Volokh, M.; Shalom, M., A General Synthesis of Porous Carbon Nitride Films with Tunable Surface Area and Photophysical Properties. *Angew. Chem. Int. Ed.* **2018**, *57* (5), 1186-1192
- 9. Yu, B.; Kim, D.; Kim, S.; Hong, S. H., Cyanuric Acid-Based Organocatalyst for Utilization of Carbon Dioxide at Atmospheric Pressure. *ChemSusChem* **2017**, *10* (6), 1080-1084.
- 10. Nagai, D.; Kuribayashi, T.; Tanaka, H.; Morinaga, H.; Uehara, H.; Yamanobe, T., A facile, selective, high recovery system for precious metals based on complexation between melamine and cyanuric acid. *RSC Adv.* **2015**, *5* (38), 30133-30139.
- 11. Wang, Y.; Zhu, X.; Huang, Y.; Zheng, C.; Gao, X., New insights into catalytic pyrolysis mechanisms and reaction pathways of urea pyrolysis on V-Ti catalyst surfaces. *RSC Adv.* **2016**, *6* (109), 108000-108009
- 12. Schaber, P. M.; Colson, J.; Higgins, S.; Thielen, D.; Anspach, B.; Brauer, J., Thermal decomposition (pyrolysis) of urea in an open reaction vessel. *Thermochim. Acta* **2004**, *424* (1), 131-142.
- 13. Sakata, Y.; Yoshimoto, K.; Kawaguchi, K.; Imamura, H.; Higashimoto, S., Preparation of a semiconductive compound obtained by the pyrolysis of urea under N2 and the photocatalytic property under visible light irradiation. *Catal. Today* **2011**, *161* (1), 41-45.
- 14. Jeilani, Y. A.; Orlando, T. M.; Pope, A.; Pirim, C.; Nguyen, M. T., Prebiotic synthesis of triazines from urea: a theoretical study of free radical routes to melamine, ammeline, ammelide and cyanuric acid. *RSC Adv.* **2014**, *4* (61), 32375-32382.
- 15. Chemat, F.; Poux, M., Microwave assisted pyrolysis of urea supported on graphite under solvent-free conditions. *Tetrahedron Lett.* **2001**, *42* (22), 3693-3695.
- 16. Tischer, S.; Börnhorst, M.; Amsler, J.; Schoch, G.; Deutschmann, O., Thermodynamics and reaction mechanism of urea decomposition. *Phys. Chem. Chem. Phys.* **2019**, *21* (30), 16785-16797.
- 17. She, D.-M.; Yu, H.-L.; Huang, Q.-L.; Li, F.-M.; Li, C.-J., Liquid-phase synthesis of cyanuric acid from urea. *Molecules (Basel, Switzerland)* **2010**, *15* (3), 1898-1902.
- 18. WPO, CN201610290445.7A, **2016**.
- 19. WPO, CN2011104107983A, 2011.
- 20. CPC, CN104961699A, 2015.
- 21. Tao, M.; Yin, Q.; Kaledin, A. L.; Uhlikova, N.; Lu, X.; Cheng, T.; Chen, Y.-S.; Lian, T.; Geletii, Y. V.; Musaev, D. G.; Bacsa, J.; Hill, C. L., Structurally Precise Two-Transition-Metal Water Oxidation Catalysts: Quantifying Adjacent 3d Metals by Synchrotron X-Radiation Anomalous Dispersion Scattering. *Inorg. Chem.* **2022**, *61* (16), 6252-6262.
- 22. Abdullayev, Y.; Rzayev, R.; Autschbach, J., Computational mechanistic studies on persulfate assisted p-phenylenediamine polymerization. *J. Comput. Chem.* **2022**, *43* (19), 1313-1319.

- 23. Wang, C.; Guo, L.; Li, H.; Wang, Y.; Weng, J.; Wu, L., Preparation of simple ammonium ionic liquids and their application in the cracking of dialkoxypropanes. *Green Chemistry* **2006**, *8* (7), 603-607.
- 24. Frisch, M. J.; Trucks, G. W.; Schlegel, H. B.; Scuseria, G. E.; Robb, M. A.; Cheeseman, J. R.; Scalmani, G.; Barone, V.; Petersson, G. A.; Nakatsuji, H.; Li, X.; Caricato, M.; Marenich, A. V.; Bloino, J.; Janesko, B. G.; Gomperts, R.; Mennucci, B.; Hratchian, H. P.; Ortiz, J. V.; Izmaylov, A. F.; Sonnenberg, J. L.; Williams; Ding, F.; Lipparini, F.; Egidi, F.; Goings, J.; Peng, B.; Petrone, A.; Henderson, T.; Ranasinghe, D.; Zakrzewski, V. G.; Gao, J.; Rega, N.; Zheng, G.; Liang, W.; Hada, M.; Ehara, M.; Toyota, K.; Fukuda, R.; Hasegawa, J.; Ishida, M.; Nakajima, T.; Honda, Y.; Kitao, O.; Nakai, H.; Vreven, T.; Throssell, K.; Montgomery Jr., J. A.; Peralta, J. E.; Ogliaro, F.; Bearpark, M. J.; Heyd, J. J.; Brothers, E. N.; Kudin, K. N.; Staroverov, V. N.; Keith, T. A.; Kobayashi, R.; Normand, J.; Raghavachari, K.; Rendell, A. P.; Burant, J. C.; Iyengar, S. S.; Tomasi, J.; Cossi, M.; Millam, J. M.; Klene, M.; Adamo, C.; Cammi, R.; Ochterski, J. W.; Martin, R. L.; Morokuma, K.; Farkas, O.; Foresman, J. B.; Fox, D. J. Gaussian 16, Revision C.01, Gaussian Inc. Wallingford CT: 2016.
- 25. Becke, A. D., Density-functional exchange-energy approximation with correct asymptotic behavior. *Phys. Rev. A* **1988**, *38* (6), 3098-3100.
- 26. Lee, C.; Yang, W.; Parr, R. G., Development of the Colle-Salvetti correlation-energy formula into a functional of the electron density. *Phys. Rev. B* **1988**, *37*, 785.
- 27. Grimme, S.; Antony, J.; Ehrlich, S.; Krieg, H., A consistent and accurate ab initio parametrization of density functional dispersion correction (DFT-D) for the 94 elements H-Pu. *J. Chem. Phys.* **2010**, *132* (15), 154104.
- 28. Chagovets, V. V.; Kosevich, M. V.; Stepanian, S. G.; Boryak, O. A.; Shelkovsky, V. S.; Orlov, V. V.; Leontiev, V. S.; Pokrovskiy, V. A.; Adamowicz, L.; Karachevtsev, V. A., Noncovalent Interaction of Methylene Blue with Carbon Nanotubes: Theoretical and Mass Spectrometry Characterization. *J. Phys. Chem. C* **2012**, *116* (38), 20579-20590.
- 29. Deguchi, Y.; Kono, M.; Koizumi, Y.; Izato, Y.-i.; Miyake, A., Study on Autocatalytic Decomposition of Dimethyl Sulfoxide (DMSO). *Org. Process Res. Dev.* **2020**, *24* (9), 1614-1620.
- 30. Wang, Y.; Liu, X.; Bai, L.; Niu, J., Influence of alkyl chain length of alpha olefin sulfonates on surface and interfacial properties. *J. Dispersion Sci. Technol.* **2017**, *38* (12), 1764-1769.
- 31. Abdullayev, Y.; Abbasov, V.; Ducati, L. C.; Talybov, A.; Autschbach, J., Ionic Liquid Solvation versus Catalysis: Computational Insight from a Multisubstituted Imidazole Synthesis in [Et2NH2][HSO4]. *ChemistryOpen* **2016**, *5* (5), 460-469.
- 32. Valiyev, I.; Abdullayev, Y.; Yagubova, S.; Baybekov, S.; Salmanov, C.; Autschbach, J., Experimental and computational study of metal-free Brønsted acidic ionic liquid catalyzed benzylic C(sp3)H bond activation and CN, CC cross couplings. *J. Mol. Liq.* **2019**, *280*, 410-419.
- 33. Wang, X.; Aldrich, C. C., Development of an imidazole salt catalytic system for the preparation of bis(indolyl)methanes and bis(naphthyl)methane. *PLOS ONE* **2019**, *14* (4), e0216008.
- 34. Muthusamy, S.; Gnanaprakasam, B., Imidazolium salts as phase transfer catalysts for the dialkylation and cycloalkylation of active methylene compounds. *Tetrahedron Lett.* **2005**, *46* (4), 635-638.
- 35. Zhao, L.; Zhang, C.; Zhuo, L.; Zhang, Y.; Ying, J. Y., Imidazolium Salts: A Mild Reducing and Antioxidative Reagent. *J. Am. Chem. Soc.* **2008**, *130* (38), 12586-12587.
- 36. Wang, D.; Dong, N.; Hui, S.; Niu, Y., Analysis of urea pyrolysis in 132.5–190 °C. *Fuel* **2019**, *242*, 62-67.
- 37. Zhang, Y.; Zhen, B.; Li, H.; Feng, Y., Basic ionic liquid as catalyst and surfactant: green synthesis of quinazolinone in aqueous media. *RSC Adv.* **2018**, *8* (64), 36769-36774.
- 38. Guo, H.; Duereh, A.; Hiraga, Y.; Aida, T. M.; Qi, X.; Smith, R. L., Perfect recycle and mechanistic role of hydrogen sulfate ionic liquids as additive in ethanol for efficient conversion of carbohydrates into 5-ethoxymethylfurfural. *Chem. Eng. J.* **2017**, *323*, 287-294.
- 39. Eichelbaum, M.; Farrauto, R. J.; Castaldi, M. J., The impact of urea on the performance of metal exchanged zeolites for the selective catalytic reduction of NOx: Part I. Pyrolysis and hydrolysis of urea over zeolite catalysts. *Appl. Catal., B* **2010**, *97* (1), 90-97.
- 40. Yang, W.; Chen, Z.; Zhou, J.; Huang, Z.; Cen, K., Catalytic Performance of Zeolites on Urea Thermolysis and Isocyanic Acid Hydrolysis. *Ind. Eng. Chem. Res.* **2011**, *50* (13), 7990-7997.